

Extremely Prolate Granular Materials

K. Stokely, A. Diaconu, and Scott V. Franklin*

Dept. of Physics, Rochester Institute of Technology

(Dated: December 2, 2024)

We investigate the two-dimensional packing of extremely prolate (aspect ratio $\alpha = L/D > 10$) granular materials, comparing experiments with Monte-Carlo simulations. In experimental piles of particles with aspect ratio $\alpha = 12$ we find the average packing fraction to be 0.68 ± 0.03 . Both experimental and simulated piles contain a large number of horizontal particles, and particle alignment is quantified by an orientational order correlation function. In both simulation and experiment the correlation between particle orientation decays after a distance of two particle lengths. It is possible to identify voids in the pile with sizes ranging over two orders of magnitude. The experimental void distribution function is a power law with exponent $-\beta = -2.37 \pm 0.05$. Void distributions in simulated piles do not decay as a power law, but do show a broad tail. We extend the simulation to investigate the scaling at very large aspect ratios. A geometric argument predicts the pile number density to scale as α^{-2} . Simulations do indeed scale this way, but particle alignment complicates the picture, and the actual number densities are quite a bit larger than predicted.

One of the more striking features of piles of very prolate granular materials (large aspect ratio $\alpha = L/D$) is the connected network that forms at comparatively low packing fractions. The formation of this network is often commercially undesirable. LCD screens, for example, cannot function if the molecules are entangled, and lumber floating down a river stops when the logs jam. There are, however, practical applications for such “jammed” networks. Piles of large aspect-ratio materials are extremely rigid, even at low packing fractions, and have a high strength:weight ratio. At the extremely small scale, networks of carbon nanotubes are a possible mechanism for conducting energy to and from nano-devices [1].

Little is known about even basic characteristics of piles formed from rod-like particles, most granular research [2, 3, 4, 5, 6, 7, 8] being limited to $\alpha < 5$. The rigidity of such piles is due to particle entanglement, with particle rotation extremely constrained. The statistics of particle orientations which determines these constraints, however, is not known. While it seems obvious that particles will align, in fact two-dimensional piles contain a number of orthogonal particles that create large voids which dominate the pile landscape (see Fig. 1). The only work above $\alpha \sim 10$ we are aware of is that of Philipse [9, 10], who formed piles of copper wire of aspect ratios ranging from 5 to 77 and explained the $1/\alpha$ scaling of the volume fraction with a simple phenomenological model. As the particles’ aspect ratio increased, they could no longer be poured from their initial container, and tended to fall out as a solid “plug”. The cause of this transition, which occurs at $\alpha \sim 35$, is not known.

To form prolate particles, acrylic rods (diameter $D = 0.16$ cm) were cut to a length $L = 1.9$ cm ($\alpha \approx 12$) and constrained between two Plexiglas sheets separated by a spacer 1.25 particle diameters thick. The uniform spacing throughout the plates prevents particles from overlapping; piles are effectively 2-dimensional. Piles are

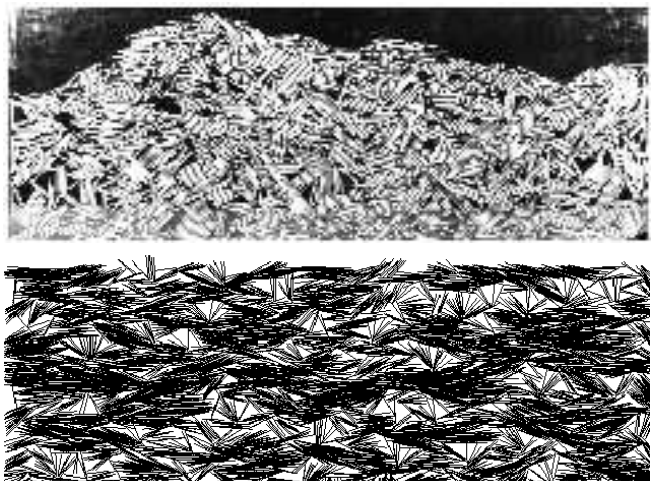


FIG. 1: **Top:** 2-d pile of $\alpha = 12$ acrylic rods backlit with fluorescent lights. The middle third of each particle appears bright. **Bottom:** Simulated pile of $\alpha = 12$ rods. Both piles show particles aligning and a wide distribution of void sizes.

formed by distributing particles at random on one Plexiglas sheet, attaching the second sheet, and slowly rotating the system to vertical. The initial distribution of rods is not truly random; local orientational correlations exist as neighboring particles are forced to be aligned (or else they would overlap). This could be avoided in principle by reducing the number of rods on the plate; in practice, however, this would be prohibitively slow. Additional rods are prepared in a similar manner in an identical cell which is used as a funnel to pour particles onto the pile. Piles formed this way are 53 cm wide, typically 25 cm high and contain about 2000 particles. A picture of a pile is shown in Fig. 1 (top). The piles are backlit with fluorescent lights. The cylindrical rods act as lenses, displaying a thin bright line throughout the middle of each rod. We have written software that identifies connected, collinear bright pixels in a picture and extracts the parti-

cle location and orientation. Data reported involve averaging over 19 separate piles. Despite the less-than-ideal preparation, piles were statistically consistent; packing fractions varied by $\sim 5\%$ and void distribution and orientational order functions were similarly reproducible.

Buchalter and Bradley[3, 4] developed a Monte-Carlo simulation for ellipsoidal particles. We adapted this for cylindrical particles and extended the aspect ratio by two orders of magnitude ($\alpha_{\max} = 1000$). Particles move along the nodes of a discrete lattice ($N \times N$, with $N \sim 10L$) and can rotate freely. Particles are placed at random locations and orientations and then move, one at a time, along randomly generated displacement/rotation paths. The only constraint on the motion is that particles cannot move upwards or overlap with other particles. If an intersection occurs, the particle is placed at its last allowable position and a new particle is chosen for an attempted move. The process repeats until the potential energy (the sum of the particle heights) remains constant for 5000 time steps, each particle unable to move for, on average, 10 attempted moves. A new group of particles is then placed above the formed pile and allowed to settle. All piles are at least 7 particle lengths high and we have checked to ensure that additional pourings do not appreciably change the pile's statistics. A sample pile is shown in Fig. 1 (bottom). The length of the particles, constant through any one pile, is varied from 10 to 1000. Results for a given aspect ratio are averaged over five piles; additional piles do not change the statistics.

The range of packing fractions achievable with 2-d disks under gravitational forces is quite narrow. The upper and lower limits are given by hexagonal ($\phi_{hcp} = 0.915$) and orthogonal ($\phi_{ocp} = 0.785$) close packing respectively [11], with the random close packing value $\phi_{rcp} \approx 0.785$. We find the average packing fraction of rods with $\alpha = 12$ to be $\phi = 0.68 \pm 0.03$. The lowest measured value was 0.63; the largest 0.72. Particles in both simulations and experiment prefer to be horizontal, although the experiment has a broader distribution about horizontal than the simulation (Fig. 2). Experimental piles also have more vertical rods than the simulation, a consequence, we believe, of friction between particles which is not incorporated in the simulation.

The appearances of simulated and experimental piles are dominated by large, but rare, voids. From the images we find the number of voids as a function of void area A . The void distribution functions $V(A)$ from experimental (\bullet) and simulated ($*$) piles are plotted vs. void area A in Fig. 3. As Fig. 3 shows, experimental void sizes vary by almost two decades. The experimental data are well-fit by a power law $A^{-2.37 \pm 0.05}$ (straight line in Fig. 3). Simulated piles show a similar decay, although the function does not seem to follow a power law. We did not notice any significant dependence of the void distribution function on the particle aspect ratio in simulated piles, although this warrants further study.

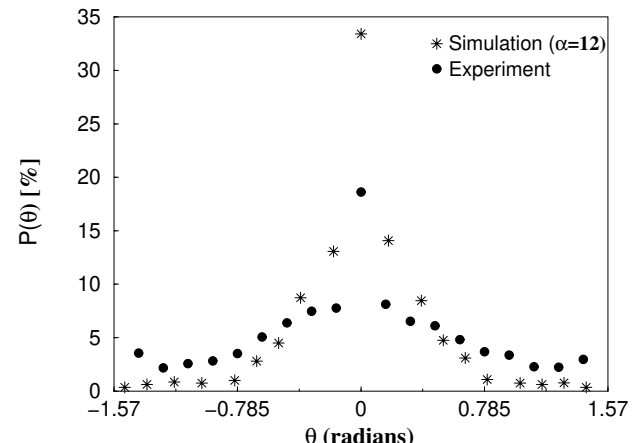


FIG. 2: Angular distribution of experimental (\bullet) and simulated (*) particles. Both show a peak about horizontal alignment ($\theta = 0$), the experiment having the broader distribution.

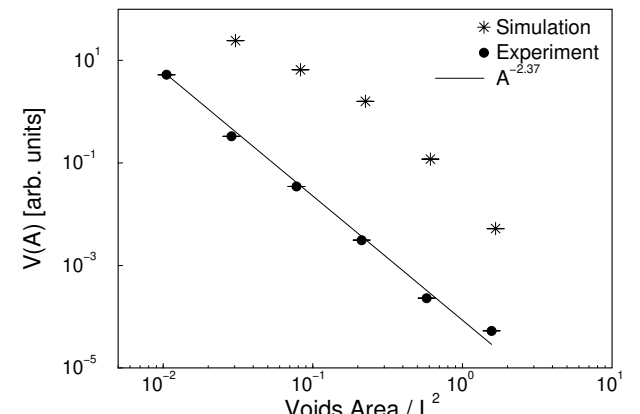


FIG. 3: Void distribution function $V(A)$ as a function of void area (scaled by particle length L squared. $V(A)$ is expressed as a percentage of the total number of voids. Voids in both experiment (\bullet) and simulation (*, with $\alpha = 20$) decay as a $A^{-\beta}$ with $\beta = 2.37 \pm 0.05$. This means that smaller voids occupy a greater total area than the larger, rarer, voids.

There are several intriguing consequences to the fact that the exponent in $V(A)$ is between -2 and -3. First, the total area taken up by all voids with size A is $AV(A) \propto A^{-1.37}$. As $\lim_{A \rightarrow \infty} [AV(A)] \rightarrow 0$, the cumulative effect of the smaller voids to the pile's area is actually larger than that of the larger voids. We also note that the total area occupied by all voids $\int AV(A)dA$ also remains finite as, in fact, it must for realistic piles. The integral for the mean square void area $\langle A^2 \rangle = \int V(A)A^2dA$, however, diverges as A goes to infinity.

Both experiment and simulation find neighboring particles aligning. This is quantified with an orientational correlation function

$$Q(r) = \langle \cos(2 * \Delta\theta_{ij}) \rangle.$$

$\Delta\theta_{ij}$ is the difference in angle between rods i and j and

the average is over all particles whose centers-of-mass separation is between r and $r + \delta r$. This function, related to an earlier orientational order parameter [3, 4], takes values ranging from 1 if particles are parallel to -1 if particles are perpendicular. Two particles whose centers-of-mass are quite close must be aligned and so $Q(r \rightarrow 0) \rightarrow 1$. Once particle centers-of-mass are separated by more than one rod length L they can in principle assume any relative orientation and so $Q(r \rightarrow \infty) \rightarrow 0$. For comparison, we calculate analytically the correlation function resulting from a distribution where rods assume all allowable angles with equal probability. This is the simplest possible ordering, the only constraint being that rods cannot overlap, and is used in simple geometric models for predicting number density. The allowable angles θ a rod can take with respect to a fixed rod assumed to lie along the x axis are found as a function of center-of-mass separation r and angle ϕ that the line connecting the centers-of-mass makes with the x axis. If the minimum/maximum allowable angles are given by θ_{min} and θ_{max} then $Q(r)$ is

$$Q(r) = \int_0^{2\pi} d\phi \int_{\theta_{min}(r,\phi)}^{\theta_{max}(r,\phi)} \cos(2\theta) d\theta.$$

Figure 4 shows the $Q(r)$ distribution resulting from the analytic (line), experimental (\bullet), and simulated ($*$) piles. Both the experimental and simulated piles show greater correlation between neighboring rods, seen in the divergence from the analytic line for $r/L > 0.5$ (between the dashed lines), and reach an asymptotic value once rods are separated by more than one or two rod lengths. The experimental correlation has a longer range, the asymptote reached only after $r/L > 2$.

The long-range correlation between particles shown in Fig. 4 does not represent a long-range influence of one particle on another, but rather results from the overall preference for particles to be horizontal. This is confirmed by calculating

$$Q(r \rightarrow \infty) = \int P(\theta)P(\phi) \cos[2(\theta - \phi)] d\theta d\phi,$$

which assumes the rod angles are drawn at random from the distribution $P(\theta)$ shown in Fig. 2. The differences in the simulation and experimental distribution functions result in $Q(r \rightarrow \infty)_{\text{exp}} = 0.16$ and $Q(r \rightarrow \infty)_{\text{sim}} = 0.53$, agreeing quite well with the asymptotic values in Fig. 4.

We now extend the simulation to larger aspect ratios and investigate the scaling of various quantities. The rigidity of a pile depends on particles in contact, hence we calculate the *contact number* $\langle c \rangle$. Fig. 5(top) shows that $\langle c \rangle$ reaches an asymptotic value of ≈ 3.2 by aspect ratio 50. This may seem counter-intuitive, as longer particles in principle can be in contact with more neighbors. Orientations that maximize $\langle c \rangle$, however, are quite rare

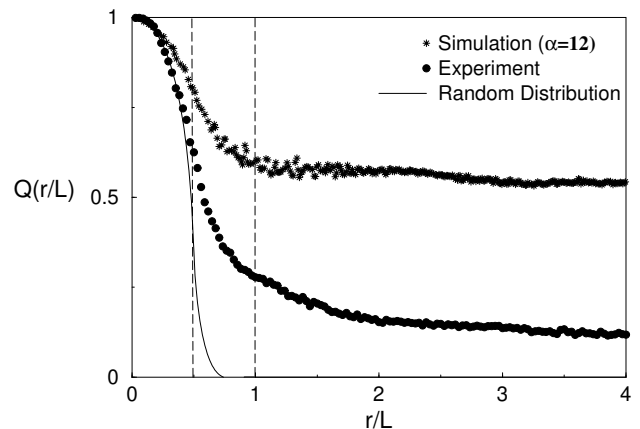


FIG. 4: Orientational correlation function $Q(r/L)$ as a function of center-of-mass separation scaled by particle length. The solid line represents the correlation resulting from a distribution where particles assume all allowable angles with equal probability. Both experiment and simulation show enhanced alignment for r/L between 0.5 and 1 (between dashed lines) but noticeably different asymptotic values due to the different angular distributions from Fig. 2.

and the length-independence of contact number is due to the tendency of neighboring particles to align and screen one another from other particles. As particle aspect ratio decreases, and the particles become more circular, this screening effect diminishes and the contact number increases. Packings of circular disks, for example, show a contact number between 4 (orthogonal close packing) and 6 (hexagonal close packing).

The pile orientational order is characterized by the order parameter $Q = \langle \cos(2\theta_i) \rangle$ where θ_i is the angle the i th particle makes with the horizontal and Q is averaged over all particles. Q ranges from 1 (all particles horizontal) to -1 (all particles vertical), with $Q = 0$ indicating a random distribution of angles (or all particles at 45°). As shown in Fig. 5, Q of simulated piles decreases as the particle length increases reaching an asymptote of 0.3. Q for experimental piles of particles with aspect ratio $\alpha = 12$ is 0.33 ± 0.05 , within the asymptotic value of simulations.

Philipse proposed the Random Contact Model[9] to explain the low packing fractions of three-dimensional piles. We now briefly apply his logic to our two-dimensional piles and show the discrepancies caused by the enhanced particle alignment described above.

The existence of one particle excludes a fraction of the possible orientations, called the *excluded area* A_{excl} , that can be assumed by a second particle. If particles are not in contact then the number density of particles is simply $\langle N \rangle = 1/A_{\text{excl}}$. In fact, each particle touches on average $\langle c \rangle$ neighbors. Applying a mean-field approximation, the

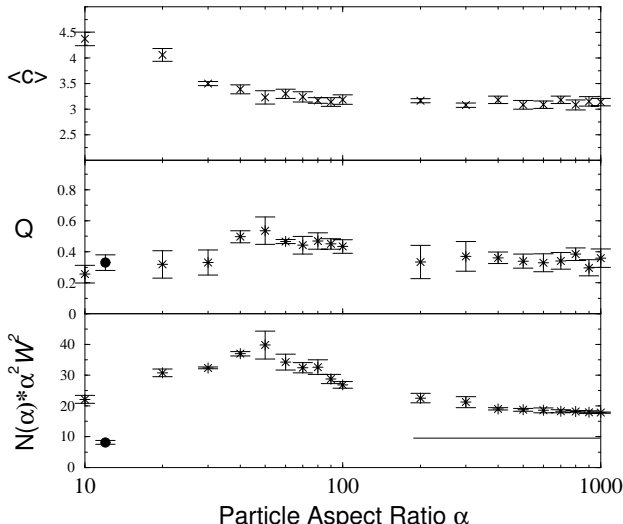


FIG. 5: **Top:** Contact number in simulated piles as a function of particle aspect ratio. As assumed in the Random Contact Model, $\langle c \rangle$ is independent of aspect ratio for long particles. **Middle:** Orientational order parameter Q as a function of aspect ratio for simulation (*) and experiment (●). **Bottom:** Number density multiplied by α^2 for simulation (*) and experiment. As predicted by the *RCM*, $N(\alpha) \sim \alpha^{-2}$. The asymptotic value of $N(\alpha) * \alpha^2$, however, is larger than that predicted by the *RCM*, a consequence of particle alignment.

number density of a connected network is

$$\langle N \rangle = \frac{2\langle c \rangle}{A_{\text{excl}}},$$

where the factor of 2 accounts for the fact that each contact involves two particles. The key assumption is that contacts are uncorrelated, i.e. particles assume all allowable orientations with equal probability. We have already shown that this assumption is not satisfied. The excluded area of a stick with length L and width W is to first order $A_{\text{excl}} = (2/\pi)L^2$ [12]. With $\langle c \rangle = 3.2$, the number density as a function of aspect ratio α is predicted to be

$$N(\alpha) = \frac{2\langle c \rangle}{(2L^2/\pi)} = C\alpha^{-2}W^{-2}$$

with $C = 10$. In Fig. 5 (bottom) we have plotted $N(\alpha)\alpha^2W^2$ as a function of α . The asymptotic horizontal line for large aspect ratios indicates that the number density does indeed scale as $1/\alpha^2$. The constant, however, is larger than that predicted by the RCM (flat line in Fig. 5 (bottom)). Piles are therefore more dense than predicted, implying that the excluded area of particles is about 33% less than that in an isotropic distribution. This is a result of particle alignment, seen earlier in Fig. 4. We also note that the scaling as α^{-2} is realized only for the largest of aspect ratios, while the constancy of contact number occurs much earlier. Finally, the experimental number density is found from the packing fraction ϕ

with $N = \phi/A_{\text{rod}} = 2.44 \text{ cm}^{-2}$. This value (multiplied by α^2W^2) is also plotted in Fig. 5 and is less than the corresponding simulation, a consequence of the simulation's greater number of efficiently packed horizontal rods.

We have presented the first quantitative characterization of two-dimensional piles formed from very prolate ($\alpha > 10$) granular materials finding, for example, the packing fraction of rods with aspect ratio $\alpha = 12$ to be 0.68 ± 0.03 . Particles separated by less than two rod lengths show a greater orientational correlation than would be found in a random pile; rods separated by more than two rod lengths are uncorrelated except for the general preference for horizontal alignment imposed by gravity. The void distribution function in experimental piles obeys a power law with exponent $-\beta = 2.37 \pm 0.05$; Monte-Carlo simulations show similar angular correlations and void distribution functions. Simulations have a greater number of horizontal rods, however, and thus produce piles with larger number densities than found in both experiment and simple geometric models.

We thank E. R. Redish for first questioning the characteristics of pickup sticks and John C. Crocker for calling attention to the work of Philipse. Eric R. Weeks and L. S. Meichle have provided invaluable advice throughout this project. Saul Lapidus and Peter Gee were involved in much of the original setup of the experiment.

* svfspd@rit.edu; <http://piggy.rit.edu/franklin/>

- [1] R. P. Raffaelle, T. Gennett, J. Maranchi, P. Kumta, M. J. Heben, A. C. Dillon, and K. C. Jones, in *MRS Bulletin Proceedings* (Materials Research Society, 2001), vol. 706.
- [2] F. X. Villarruel, B. E. Lauderdale, D. M. Mueth, and H. M. Jaeger, *Phys. Rev. E* **61**, 6914 (2000).
- [3] B. J. Buchalter and R. M. Bradley, *J. Phys. A* **25**, L1219 (1992).
- [4] B. J. Buchalter and R. M. Bradley, *Phys. Rev. A* **46**, 3046 (1992).
- [5] J. R. Williams and G. W. Mustoe, in *Computers and Geotechnics* (Elsevier Applied Science Publishers Ltd., 1990).
- [6] G. G. W. Mustoe, M. Miyata, and M. Nakagawa., in *Finite Elements: Techniques and Developments* (Civil-Comp Press, 2000).
- [7] P. W. Cleary and M. L. Sawley, *Applied Mathematical Modeling* **26** (2002).
- [8] I. C. Rankenburg and R. J. Zieve, *Phys. Rev. E* **63**, 061303 (2001).
- [9] A. Philipse, *Langmuir* **12**, 1127 (1996).
- [10] A. P. Philipse and A. Verberkmoes, *Physica A* **235**, 186 (1997).
- [11] D. Howell and R. P. Behringer, *Phys. Rev. Lett.* **82** (1999).
- [12] I. Balberg, C. H. Anderson, S. Alexander, and N. Wagner, *Phys. Rev. B* **30**, 3933 (1984).